ELSEVIER

Chemical Geology 214 (2005) 193–208

CHEMICAL GEOLOGY
INCLUDING
ISOTOPE GEOSCIENCE

www.elsevier.com/locate/chemgeo

Speleothem organic matter content imaging. The use of a Fluorescence Index to characterise the maximum emission wavelength

Yves Perrette[a,*], Jean-Jacques Delannoy[b], Marc Desmet[c], Vincent Lignier[b], Jean-Luc Destombes[d]

[a]*Laboratoire de Géographie Physique, UMR 8591, Campus de Bellevue, 92195 Meudon Cedex, France*
[b]*Environnement, Dynamique et Territoires en Montagne, Campus Scientifique, Savoie Technolac, F73376 Le Bourget du Lac, France*
[c]*Laboratoire de Géodynamique des Chaînes Alpines UMR 5025; Campus Scientifique, Savoie Technolac, F73376 Le Bourget du Lac, France*
[d]*Physique des Lasers Atomes et Molécules, UMR 8523, Université Scientifique et Technologique de Lille, F59100 Villeneuve d'Ascq, France*

Received 28 October 2003; accepted 27 September 2004

Abstract

The study of palaeoenvironments, especially pedologic and biologic environments, is fundamental to a complete understanding of continental climate changes. Many types of sediment contain organic molecules (OM) that were trapped during the depositional process, with the quantity and the nature of these organic molecules being strongly influenced by climate and other local factors. The quantity of organic matter in sediment can be measured by fluorescence intensity, but its nature is more difficult to determine. For this research, the organic molecules in stalagmites were analysed using emission fluorescence spectroscopy. The analysis of carbonated karst sediments was complemented by studies of clay, soil and seepage water samples. The main objective of this paper is to describe a method for the continuous imaging of the spectroscopic features of stalagmite organic molecules. Continuous imaging provides a means of circumventing the nonlinearity, both in space (of the sediment) and in time (of the sedimentation process), of the trapping of organic matter.

This methodological report presents a protocol for calculating a Fluorescence Index (FI) that can be used in palaeoenvironmental studies of sediment. A similar approach to that used for determining E4/E6 ratios was used to determine the ratio of the fluorescence intensities of a sample at 514 nm and at 456 nm. This Fluorescence Index is strongly correlated to the wavelength of the maximum intensity of the organic matter spectrum. Due to the relatively stable chemical environment of calcite growth, changes in the Fluorescence Index can be interpreted as being due to changes in the nature of the organic molecules rather than to pH or quenching effects. As an illustration of how this index can be used, we present some examples of fluorescence indices for speleothem samples that show short-term and long-term environmental changes. To allow fuller

* Corresponding author.
E-mail address: yves.perrette@univ-savoie.fr (Y. Perrette).

doi:10.1016/j.chemgeo.2004.09.002

palaeoenvironmental interpretations to be made, fluorescence indices need to be calibrated to environments and samples need to be dated.

Keywords: Stalagmite; Organic matter; Spectroscopy; Laser; Karst; Imagery; E4/E6

1. Introduction

Since the early 1990s, an increasing number of speleothem records have been published and they are now commonly used in the study of continental climate and environment change (Baker et al., 1993; Frappier et al., 2002; Genty et al., 2002; Genty and Quinif, 1996; Lovlie et al., 1990). Speleothem growth is controlled by climate (water and temperature) and environment (CO_2 supplied by the vegetation) (Ford and Williams, 1989; Hill and Forti, 1997); therefore, the particles and molecules trapped during precipitation reflect the palaeoenvironment (Gascoyne, 1992; Quinif, 1992; Van Beynen et al., 2001). This paper focuses on the study of these types of record in speleothems.

The organic molecules (OM) trapped in speleothem crystals provide good indicators of environmental change. Studies of these organic molecules often employ similar methods to those used in the discontinuous sampling of calcite for isotopic analyses (Berstad et al., 2002; Genty et al., 2001; Genty et al., 2002; Goede, 1994; Hendy, 1971; Lovlie et al., 1990; McDermott et al., 1999; Murton et al., 2001; Spotl and Mangini, 2002; Verheyden et al., 1999) or for spectrometric studies of the trace organic or mineral contents of stalagmites (Baker et al., 1996; Perrette et al., 2000; Ramseyer et al., 1997; Rousseau et al., 1993; White and Brenan, 1989).

The discrete analysis of organic molecules is based on two major assumptions which are not necessarily valid:

- The transfer, in time and in space, of organic matter from soils to stalagmites is linear (Perrette et al., 2001; Van Beynen et al., 2000).
- The spatial distribution of inclusions of OM in stalagmites is homogenous (improbable due to the complexity of calcite crystal growth).

These two assumptions need to be confirmed by OM measurements in the field (Van Beynen et al., 2001; Van Beynen et al., 2000), by detailed studies of the presence of OM in stalagmites, and by hydrogeochemical modelling of stalactite feed waters.

As a complement to discontinuous studies, continuous imaging methods have been developed to detect changes in calcite trace element content across the speleothem. Although very precise, some of these methods have limited applications due to the small size of the surface studied (a few hundred microns; Kuczumow et al., 2003; Roberts et al., 1998). For studies of OM, continuous measurement of fluorescence intensity (Baker et al., 1993; Perrette et al., 1999; Perrette et al., 1997; Shopov et al., 1994) is a broad environmental proxy that depends on the quality and quantity of the OM, as well as on the optical characteristics of speleothem crystals (hydrochemically controlled).

The aim of this paper is to present a combination of discontinuous spectrometric, spatially resolved analysis of OM in calcite and continuous fluorescence imaging. This technical report is the first step of a project to map the quantity and nature of OM in vertical polished sections of stalagmite.

2. Theoretical approach

2.1. Short review of the fluorescence of organic matter

The term "organic matter" covers the whole family of organic molecules, including humic acids and fulvic acids. Generally, OM from speleothems are considered to be fulvic acids, i.e., water soluble (Ramseyer et al., 1997; White and Brenan, 1989). However, this assumption does not always hold true due to the complexities of karst materials and water transfers. We have used humic/fulvic terminology for chemically extracted organic molecules (Schnitzer and Khan, 1978).

White (1981) attributes the UV fluorescence of speleothems to organic matter fluorophores. Fluores-

cence intensity banding is primarily determined by the quantity of OM, and to a lesser degree by the type of OM. The OM supplied by runoff water sunk in the karst and by seepage water will have different degrees of hydrophilicity and thus present different fluorescence intensities. (Jones and Indig, 1996; Kang et al., 2002; Mazhul et al., 1997; McGarry and Baker, 2000; Peuravuori et al., 2002; Senesi et al., 1991; Zech et al., 1997). Every stalagmite location within a cave is subject to its own specific karstic drainage regime (Perrette, 2000). Therefore, the OM content of a stalagmite is dependent on its location (soil and vegetation, hydrologic events, and transfer and storage of OM in the karst). Fluorescence banding has been widely used to study the annual resolved lamination (Baker et al., 1993; Genty et al., 1997; Perrette et al., 1999; Shopov et al., 1994); however, fluorescence intensity is only one aspect of the stalagmite OM fluorescence palaeoenvironmental record. This paper presents a methodology for describing the spectroscopic features of speleothem fluorescence.

2.2. Maximum wavelength of fluorescence emission–λ_{max}

The broad spectrum of OM fluorescence emission has been described by chemists in the fields of pedology, hydrology and oceanography (Chen et al., 1977; Mazhul et al., 1997; Peuravuori et al., 2002). Fig. 1 shows three characteristic emission spectra for speleothems, cave waters and lake clay sediments (see next section for methods and sample descriptions). The shapes and wavelengths of these spectra are similar to those observed for fulvic and humic fractions (Cook and Langford, 1995; Donard et al., 1989; Hayase and Tsubota, 1985; Jones and Indig, 1996; Mazhul et al., 1997; Miano and Senesi, 1992; Ramseyer et al., 1997; Senesi et al., 1991; Zepp and Schlotzhauer, 1981). According to the literature, different functions can be fitted to such spectra to distinguish the typical OM fluorescence from the OH Raman line (Fig. 2):

- The OH stretching vibration Raman line fit is obtained using two Gaussian functions for solutions and one Lorentzian function for solid samples (Schrader, 1989).
- The broad structure of the spectrum is fitted using 4-parameter lognormal shape functions (Aitchison and Brown, 1969). The lognormal function is acknowledged to be by far the best function for fitting broad, structureless molecular bands of complex organic molecules (Maroncelli and Fleming, 1987; Siano and Metzler, 1969). For the samples studied, one lognormal fits the data with a

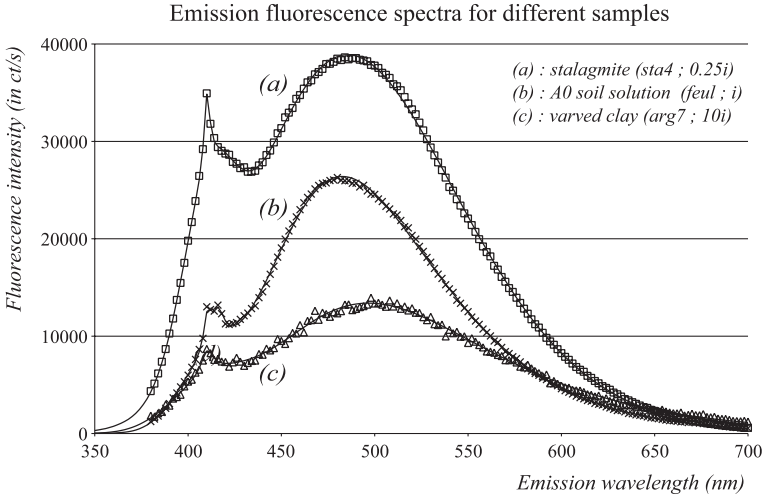

Fig. 1. Emission fluorescence spectra for different samples. Legend: see in figure.

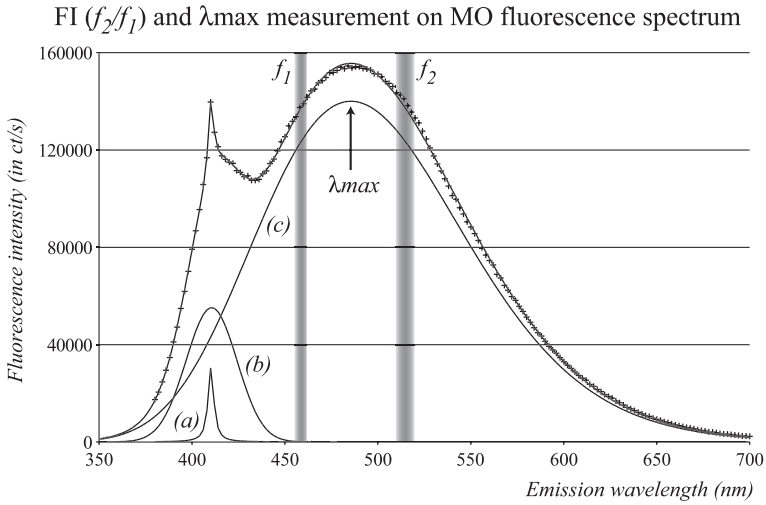

Fig. 2. Fluorescence Index and λ_{max} measurement on MO fluorescence spectrum. λ_{max}: wavelength of the maximum intensity of theoretical fluorescence (deconvolution lognormal curve); λ_{peak} : wavelength of the peak of the emission fluorescence spectrum measurement; f_1: band pass filter centred at 457 nm; f_2: band pass filter centred at 514 nm; (a) Raman lorentz deconvolution; (b) Lorentz fluorescence deconvolution; (c) Lognormal organic matter fluorescence deconvolution; λ_{max} is estimated on this curve.

square correlation coefficient (R^2) better than 0.995 (Fig. 2). Previous work (Jones and Indig, 1996) has shown that they can be ascribed to OM fluorescence.

Despite a lack of spectral details in such broad fluorescence spectra, the study of numerous samples provides an insight into the nature of the fluorescent molecules. For a given chemical environment (ion quenching, pH effects), the wavelength of the peak emission of the main lognormal curve is related to the type of OM. This calculated value is referred to as λ_{max}. λ_{max} varies between 470 and 500 nm for a 365-nm excitation wavelength and is dependent on the origin of the sample.

Given the above assumption, changes in λ_{max} are primarily induced by the molecular type of the OM, particularly its molecular weight (MW; Mazhul et al., 1997; Senesi et al., 1991; Zech et al., 1997). A blue shift in λ_{max} indicates relatively small molecules, such as FAs, whereas bigger molecules, such as HAs, produce a red shift in this spectral parameter (Jones and Indig, 1996). The shapes, size and structure of OM are discussed in an issue of Soil Science introduced by Clapp and Hayes (1999). Thus, the λ_{max} value is linked to humification (degradation/condensation of OM in soil).

However, it must be noted that λ_{max} shifts could be induced by changes in the chemical environment of the OM without a change in humification. OM spectral characteristics can be modified by variations in their chemical environment:

- pH,
- calcium concentration,
- metal ion complexing.

According to the literature, the calcium-saturated chemical environment of calcite growth means that, especially in alpine areas, the main shift in λ_{max} wavelength can be attributed to the influence of pedology on OM, and quenching and binding effects can be considered to be negligible (Borsato, 1997; McGarry and Baker, 2000; Miano and Senesi, 1992; Mobed et al., 1996; Ramseyer et al., 1997; Senesi et al., 1991; Van Beynen et al., 2000). The continuous measurement of λ_{max} in stalagmites should therefore reveal changes in soil humification. These humification changes can be induced by long-term changes in the vegetation and the soil (Genty et al., 2001), as well as by short-term climate factors, such as temperature (Christ and David, 1996) and/or rainfall (Martin-Neto et al., 1998). Due to the complexities of the relationship

between karstic drainage and soils (Bruckert and Gaiffe, 1989; Bruckert and Gaiffe, 1990; Gaiffe and Bruckert, 1985) and of humification (degradation/condensation) and its impact on the molecular weight of OM, analyses of spectrometric signatures from present-day speleothem environments have to be performed before any palaeoenvironmental interpretations can be made.

The aim of this study is to show that if there is a strong correlation between a simple global Fluorescence Index (FI) and the λ_{max} spectroscopic pattern, it will be possible to carry out continuous imaging of this spectroscopic character. The simple Fluorescence Index is determined in a similar way to the E4/E6 absorbance ratio (Chen et al., 1977; Stevenson, 1994).

3. Method and samples

The study was carried out in two stages. The first stage involved measuring the spectroscopic characteristics of the OM in soil solutions and in solids (carbonated and noncarbonated sediments) in order to be able to apply the water solution E4/E6 absorbance ratio (Chen et al., 1977; Stevenson, 1994) to a fluorescence ratio for solids. The second stage applied this Fluorescence Index to stalagmites.

The location and description of the solution and solid samples used in these two stages are shown in Table 1. This table also summarises the results used to calculate the index. To study OM from soil, we used a simple water elution process. A0 soils horizons were sampled for different soil and vegetation types (deciduous to coniferous) on a karstic plateau in the Vercors massif. Samples were eluted in distilled water at room temperature (20 °C) for 1 h. The elutions were then filtered through a DURIEUX glass fibre filter (n°28) and stored, away from sunlight, at around 6 °C.

Such extractions closely reproduce the natural behaviour of water-OM circulation through soils and karsts. The A0 horizons were collected in the Vercors Mountains, above the "Grottes de Choranche", at altitudes of between 1000 and 1400 m a.s.l., from soils under spruce, beech and box trees. Many karst dynamics studies have been undertaken in this area (Delannoy et al., 1999). Fig. 3 shows the location of the sampling points in the Choranche karst. The samples were taken from under 300 m of Urgonian limestone, near the entrance to the cave, inside and outside the area where decompression occurs.

Measurements were taken by exciting the samples with the same UV laser source (λ_{exc}=365 nm) used for fluorescence imaging. The spectrum was obtained using a double monochromator (Jobin-Yvon, U 1000) fitted with a cooled photomultiplier (Thorn EMI, 9863-S20). The spectral resolution was set to 1 nm and the signal to noise ratio was generally better than 100.

The second stage of the study involved using three major elements of the imaging protocol developed for reflectance/fluorescence imaging (Fig. 4):

- Bichannel measurements allow two different wavelengths to be scanned simultaneously. The two measurements can be reflectance and fluorescence, but for this study, two fluorescence wavelengths were used to allow a Fluorescence Index to be calculated.
- Semiconfocal measurements were used to obtain the accurate spatial scans this type of work requires. The shape and the size of the aperture placed in front of the photomultiplier opening determine the spatial resolution. For these measurements, two different apertures were used: a 50-μm slit and a 300-μm iris for high- and low-resolution scans, respectively. These sizes and shapes were chosen to optimize the signal to noise ratio with respect to the spatial measurement. Iris apertures allow a number of laminae to be measured simultaneously, whereas slit apertures give more accurate data on a smaller area. For this semiconfocal measurement, it is important to distinguish between the focalisation of the excitation and that of the scan. This colinearity (defocalisation) of the laser beam reduces the energy dissipated in the calcite OM.
- The 45° incidence of the excitation beam reduces the specular reflection noise and the energy dissipated in the calcite OM.

The vertical polished section of the stalagmite was placed on the horizontal translation table and scanned at a minimum interval of 5 μm for a

Table 1
Sum-up of sample features (location, spectroscopic and ages)

Location	Name	Type	Sample	λ_{max}	LIFI	Observation
Antre de Vénus cave, Vercors	AV9801	Translucent light brown compact calcite	sta13	482.07	1.197	Subactual
		Translucent light brown calcite	sta14	483.6	1.249	8 cm from the top (growth rate, 60 μm/year)
		Translucent light brown calcite	sta15	482.19	1.241	Between two discontinuities
		Translucent light brown calcite	sta16	480.79	1.221	Bottom of the sample (17 cm from the top)
	AV9802	Light brown compact translucent calcite	sta1	491.12	1.437	1000–1300*
		Compact translucent calcite	sta2	481.71	1.200	Older than 1000 (discontinuity)
		Compact translucent calcite	sta3	478.08	1.114	Subactual
Gouffre Berger, Vercors	BE9704	Brown caramel calcite, porous zone	sta4	484.72	1.293	Subactual
		Brown caramel calcite, compact zone	sta5	485.71	1.271	1000–1500**
	BE9703	Compact laminated calcite	sta7	484.81	1.305	Subactual
		Compact laminated calcite	sta8	475.14	1.084	800–1000*
		Compact laminated calcite	sta9	487.22	1.363	10,000 (±1500)**
		Compact laminated calcite	sta10	478.45	1.156	56,000 (±5800)*
	BE9702	Dendritic calcite with inclusions, white zone	sta11	497.12	1.606	Historic period
		Dendritic calcite with inclusions, dark zone	sta12	491.94	1.438	Historic period
	BE9706	Porous calcite with inclusions	sta17	495.73	1.460	No dates
Burbanche cave	BUR9801	Compact translucent calcite	sta19	480.47	1.232	Subactual
		Fibrous translucent calcite	sta21	492.99	1.426	Discontinuity
Gournier cave	GOU9601	Compact translucent calcite	sta22	478.57	1.133	Subactual
		Compact translucent calcite	sta23	477.42	1.114	1800–2200*
		Compact light brown translucent calcite	sta24	474.65	1.077	16000 (±1000)**
Choranche cave, Vercors	CHO9602-F	Brown compact laminated calcite	sta25	485.33	1.323	8000 (±1000)*
		Acicular calcite	sta26	487.29	1.391	7200 (±800)*
	CHO9602-A	White translucent calcite	sta29	473.63	1.066	Subactual
		Calcite with charcoal inclusions	sta30	479.32	1.191	1800 (±50)**
		Calcite with layer of charcoals and clays	sta31	483.24	1.233	1650 (±50)**
Portalerie cave, Causses	POR9701	White compact calcite	sta27	477.54	1.108	Ante-holocen
		Compact calcite with charcoals	sta28	473.8	1.066	Holocen
Izsyk-Kul lake, Kirghistan	box core XXX	Light band	arg7	496.87	1.564	(Only two samples
		Dark band	arg8	496.74	1.552	are described, they show all the same LIFI and λ_{max})
Plateau des Coulmes solutions	O horizon infusion	Decidous trees (beech essentially)	feuc	479.75	1.730	Short infusion
			feul	482.99	1.797	Long infusion
		Coniferous trees	resc	484.54	1.929	Short infusion
			resl	487.92	2.077	Long infusion
	A horizon	Box tree	solc	483.83	1.835	Brown soil
			soll	490.38	2.132	

Table 1 (*continued*)

Location	Name	Type	Sample	λ_{max}	LIFI	Observation
Choranche cave water	Chevaline network	"Cathedrale" chamber lake	hum3	477.92	1.521	Volume in the range of 1000 m^3, feeded by the Chevaline subterranean river
		Black flowstone	hum4	477.85	1.593	
		Massive stalagmite feeding	hum5	476.07	1.530	
		Lateral source	hum7	475.17	1.543	Red-brown flowstone
	Coufin network	Coufin river	hum2	472.65	1.466	
		Entrance lake	hum8	474.45	1.515	

* Age evaluated by laminae counting.
** Age evaluated by laminae counting and U/Th ages.

maximum amplitude of 30 cm (Ealing, 53-8116/6). The excitation time of 100 ms for each measurement point is controlled by the Labview (1999) computer software.

4. Fluorescence Index calculation

The E4/E6 absorbance index procedure (Chen et al., 1977; Stevenson, 1994) was used to look for a

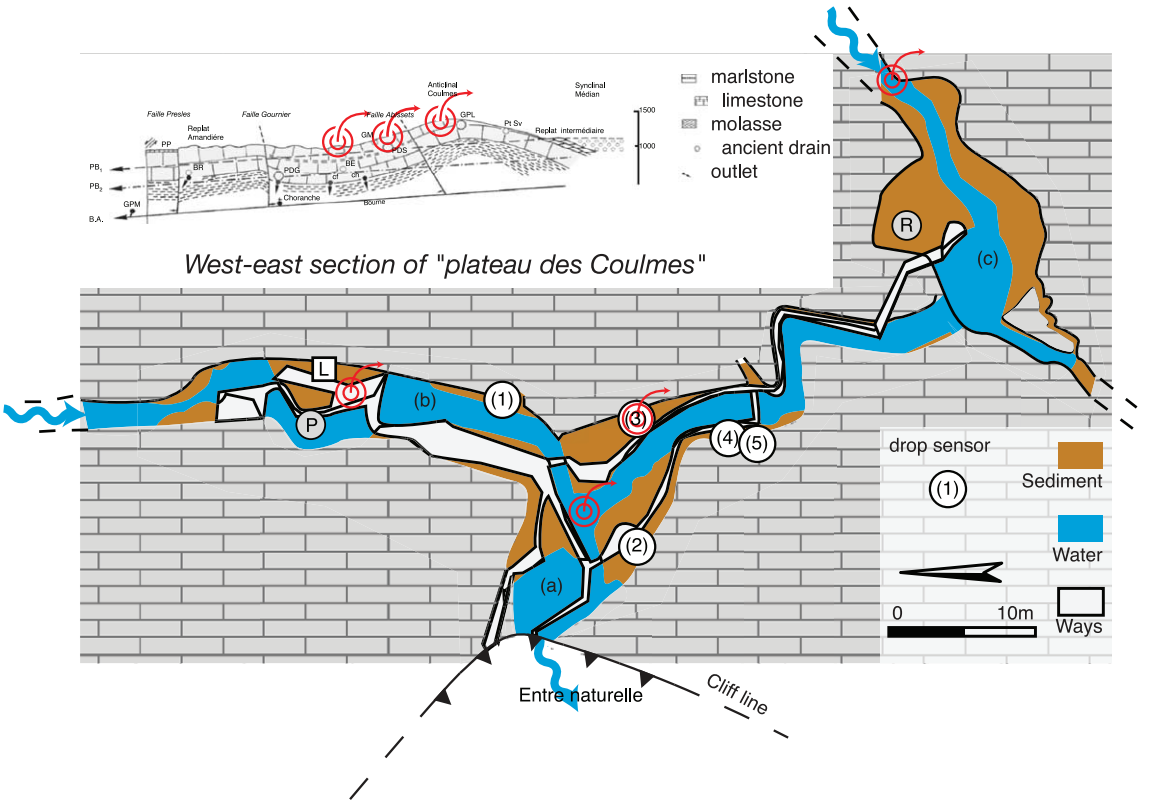

Fig. 3. Location of samples and monitoring in Choranche Cave. Legend: Red arrow symbols show the location of water and soils sampling, for monitoring, see in figure. (For interpretation of the references to colour in this figure legend, the reader is referred to the web version of this article.)

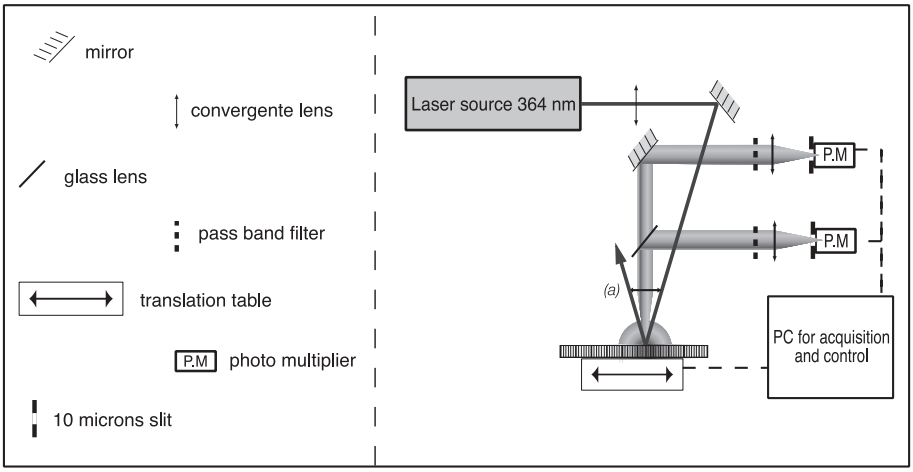

Fig. 4. Fluorescence Index imaging experimental set. Legend: see in figure.

relationship between the ratio of the fluorescence intensities at two different wavelengths and the value of λ_{max} as determined from the main lognormal fitted curve. The use of the fitted curve [ascribed to OM, cf. (c) in Fig 2] should limit the differences induced by the Raman line for a given OM environment (calcite, water or clay). We expected to find such a relationship as the shape of a normalised lognormal curve is defined by only three parameters. Taking into account the variation interval of λ_{max} in our sample set ($\approx$470 to 500 nm), a preliminary study showed that the best results were obtained by taking the ratio of the fluorescence intensities at $\approx$450 and $\approx$520 nm. The Fluorescence Index was calculated from the experimental spectra at wavelengths corresponding to commercially available optical filters centred at 457 and 514 nm (Coherent).

Fig. 5 shows the linear regression between Fluorescence Index (FI) and λ_{max} characterised by an R^2 coefficient of 0.97 for both solutions and solids. FI is the ratio of the 514- and 457-nm fluorescence intensities. To take into account the different gains of the two measurement channels and the opening of the two-band pass filters, the FI was corrected using a 1/2.967 correction factor. A clear differentiation was observed between water and solid samples, confirming that OM are not contained in fluid inclusions.

4.1. Solution samples

The distinction between cave, deciduous and coniferous waters has been defined by Sanger et al. (1997). Nevertheless, these relationships must be analysed with caution. In fact, the sample set was not large enough to allow us to take into account the role of soils (type and moisture) in humification. Furthermore, the A0 water elution assumes that infiltration is dominated by runoff waters rather than soil seepage waters. It must be noted that, for this sample set, the low Fluorescence Index for the cave water seems to indicate a filtering effect by the karst system. A more complete hydro-chemical study is in progress.

4.2. Solid samples

For the solid samples, we noted a marked difference between the λ_{max} and FI values for the lake clay sediments from Lake Issyk-Kul, a high-altitude lake in Kirghistan, and from the speleothem. As the mean elevation of Lake Issyk-Kul's catchment area is around 3800 m (Giralt et al., 2002), the humification efficiency will be low. As a result, the organic molecules in this alpine area will have high molecular weights and thus high λ_{max} and FI. The low intensity and short duration of biologic activity in such a cold environment restricts the initial degradation of vegetal macromolecules. Abiotic aggregation can therefore be considered to be negligible. On the other hand, speleothem growth requires efficient pedologic CO_2 production. Speleothem growth is associated with high humification. In the Vercors, where soils are very thin and calcium-

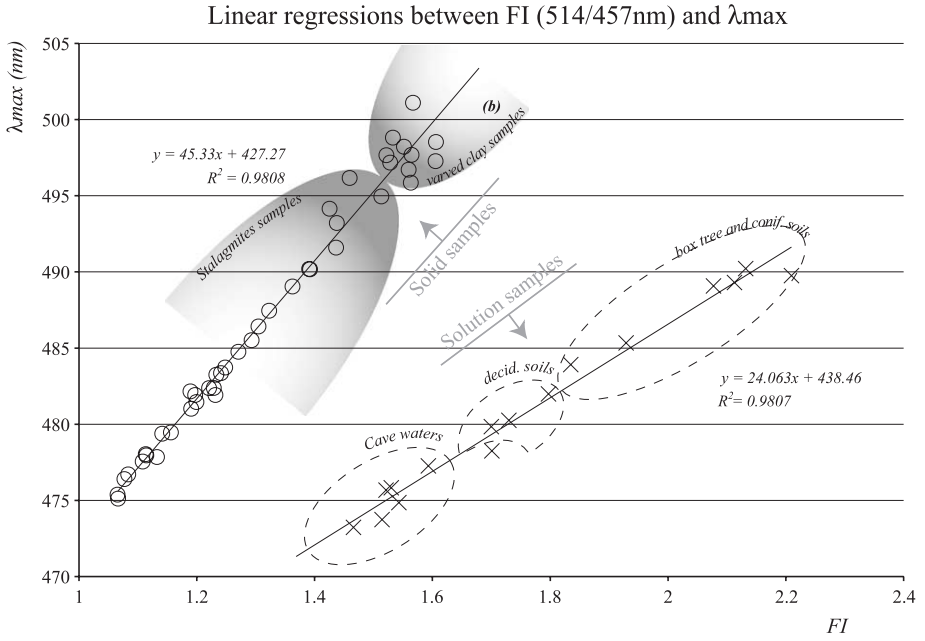

Fig. 5. Linear regression between Fluorescence Index (514/457 nm) and λ_{max} (λ_{exc}=364 nm).

saturated, the processes of OM supply are largely related to the runoff of water through poorly humified and very mobile organic matter. This produces relatively low MW material with low λ_{max} and FI. Synthesised calcite doped with a commonly used, commercially available high-MW HA (Aldrich) has a λ_{max} of around 520 nm; a much higher value than that observed for natural calcite deposits containing low-MW water-soluble molecules. The low solubility of the high-MW molecules observed in clay sediments and the geometry of stalactite drains could also explain why speleothems fed by infiltration water contain low amounts of such molecules (Baker and Brunsdon, 2003; Baker and Genty, 1999; Borsato, 1997; Destombes et al., 1997; Fenart, 2002; Genty and Deflandre, 1998; Van Beynen et al., 2000).

The measurements on solid and solution samples, which were taken on different stalagmite samples from the Vercors, show the relevance of FI imaging. The results presented below are given simply to illustrate the potential of the process and to show the technical validity of FI measurements. They are not directly usable for palaeoenvironmental reconstructions.

5. Application to stalagmites and comparison with other laser-induced images

5.1. FI imaging protocol

As a Fluorescence Index is a ratio of two values, these two values must be measured under exactly the same experimental conditions (it is especially important to use the same photomultiplier and detection chain gains). To ensure this is the case, the same channel (the detection linearity of which has been carefully checked) is used to measure successively the 457- and the 514-nm fluorescence. The second channel is used to record the reflectance of the sample for comparison. For each FI determination, three successive scans are made, two with the same optical filter (e.g., 514 nm) and the third with the other filter (e.g., 457 nm).

This allows us to calculate a blank scan in order to check the experimental reproducibility [e.g., $I_1(514)/I_2(514)$]. This blank scan should give a nearly constant value very close to 1. Because of the decrease in fluorescence time, the blank scan value is always less than 1. The Fluorescence Index does not decrease simultaneously with the decrease of fluo-

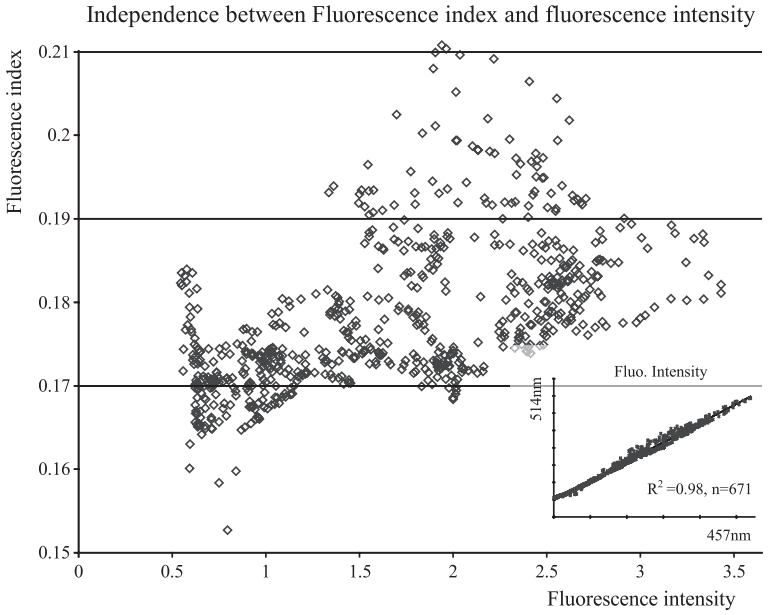

Fig. 6. Independency between Fluorescence Index and fluorescence intensity. Note: the small illustration shows the relation between the two fluorescence wavelengths.

rescence intensity. Furthermore, for stalagmite samples at 365 nm, fluorescence decrease is reversible after about 24 h. It must be noted that this "blank" scan could be analysed to give spectroscopic information on fluorescence decay (Chen et al., 2003; Clark et al., 2002; Lepane et al., 2003). Real-time

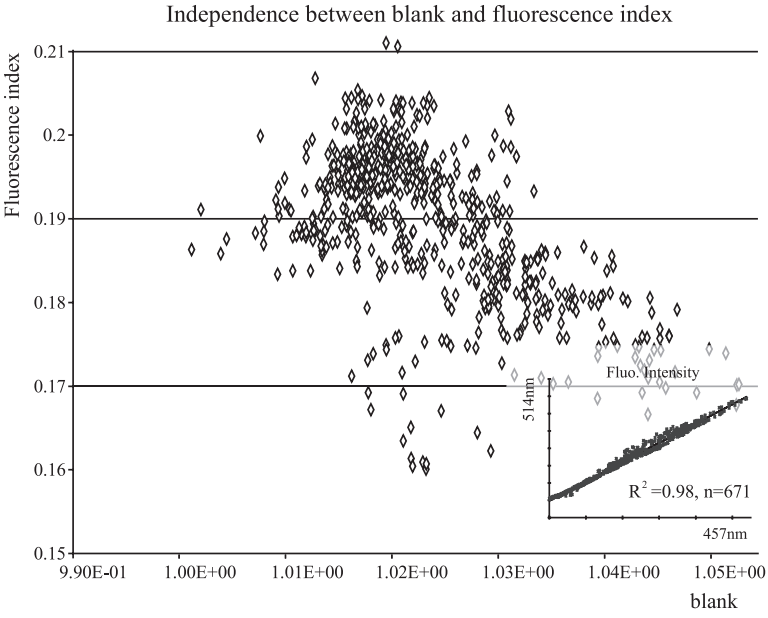

Fig. 7. Independency between Fluorescence Index and blank index. Note: the small illustration shows the relation between the two fluorescence wavelengths.

experimental sets are required to enable more complete studies of blanks to be made; something that may be developed soon.

5.2. Independence of FI from other imaging parameters

It is important to check that the FI value is independent from the blank scan and fluorescence intensity. Figs. 6 and 7 show that these imaging parameters are independent. The very weak correlation (<0.2) is not significant.

To complete this test, Fig. 8 shows that fluorescence–reflectance and FI scans are independent. The sample concerned came from the prehistoric *Grotte Chauvet* (Ardèche, France). It presents a marked delineation between a compact calcite upper part, dominated by a Dark Compact Lamination (DCL; a in Fig. 8), and a lower part (b) dominated by a White Porous Lamination (WPL; Genty et al., 1997; Genty and Quinif, 1996). The variation in the crystalline fabrics is reflected in macroscopic changes in the colour, as well as by a sharp reflectance change at the boundary between the two parts. There is a similar change in the fluorescence, which reveals a sudden decrease in the amount of organic matter involved in fluorescence (combination of the amount of OM and of the optical characteristics of calcite). The FI image (FI in Fig. 8), despite presenting variations characterised by a standard deviation of 2.5%, shows a stationary first order of λ_{max} (mean) and a differentiation in the stationary second order (standard deviation). Our objective is to describe the possibilities offered by Fluorescence Index imaging, not to interpret this specific palaeoenvironment.

FI image, independence between FI and optical structure

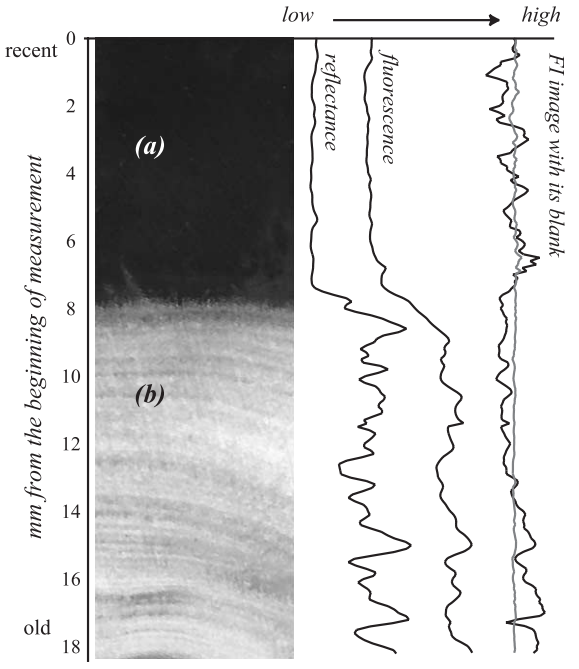

Fig. 8. Independence between Fluorescence Index scan and optical structure. (a) Compact translucent calcite; (b) White porous calcite, the microscopic colour of this zone is the same than in zone (a). FI axis is discontinue, FI values are calibrated.

6. Discussion and further work

Fluorescence indices are precise measurements that allow complementary data to be extracted from speleothem records. The following two paragraphs discuss the possibility of inferring environmental changes from stalagmites over two different time scales. Again, we present these examples as illustrations rather than as interpreted stalagmite records.

6.1. Records of changes over long time scales

Fig. 9 shows a scan of a stalagmite extracted from the Gouffre Berger. Taken from a cave that lies below 300 m of urgonian barremo–bedoulian limestone, this 30-cm-long stalagmite shows a continuous laminated growth. The base of the stalagmite was dated using the alpha U/Th method (Table 2). Ages determined by manual and computer-assisted counting of the laminae are in accordance with the radiometric age. The only objective of this time function is to give an idea of the growth time for the top 10 cm of the stalagmite, which shows a marked decrease (around 60 mm) in the Fluorescence Index from the bottom to the top. There is no associated change in the fluorescence intensity or the growth morphology. The Fluorescence Index is uniformly low along the length of the stalagmite until the top 15 mm are reached, where it increases significantly.

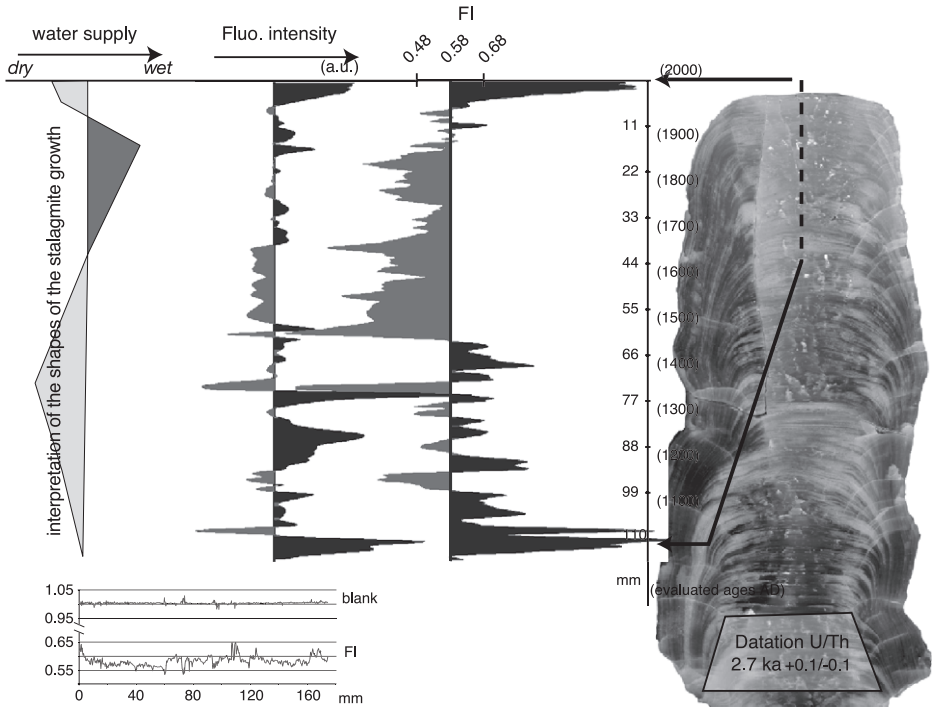

Fig 9. Example of Fluorescence Index changes in a stalagmite from the Vercors. Note that ages are evaluated by laminae counting and U/Th alpha radiometric ages. Three proxies are shown (from left to right): the relative moisture given by the shape of stalagmite growth, the fluorescence intensity and the Fluorescence Index.

In the uppermost millimetre, this increase could be due to an experimental bias induced by the fluorescence decrease (as discussed above).

Such a scan could be interpreted as evidence for a quick and durable environmental change on the Sornin Plateau (North Vercors). The decrease in FI seems to indicate a change from high to low molecular weight which could correspond to the deforestation of the Vercors during the 16th to 19th centuries.

Beyond these environmental interpretations, the relevance of this FI scan is it gives a space (i.e., time)-resolved scan that describes both a quick change and a durable effect on the environment.

6.2. High-resolution FI evolution

Some stalagmites have been scanned in order to measure FI changes within laminae. For standard low lamination rate stalagmites (inferior to 100 μm in the Alps), we have not detected any FI variations within laminae. This may be due to a true stability of the OM supply to the stalagmites scanned (buffering of soils and epikarst), or it may be that variations were below the resolution limit of the experimental method. To confirm this apparent stability in FI, these measurements will be compared with other measurements made using a different laser source (e.g., He/Cd laser at 325 nm).

Table 2
Isotopic ratio for "Gouffre Berger" stalagmite (from CERAK, Y. Quinif); both analyses correspond to the base of the stalagmite

Sample	[U]ppm	$^{234}U/^{238}U$	$^{230}Th/^{234}U$	$^{230}Th/^{232}Th$	$^{234}Th/^{238}U$	Age (ky)
Berger01a	2.076±0.02	1.348±0.008	0.026±0.002	12±4	1.350	2.8(+0.3/−0.2)
Berger01b	2.08±0.02	1.345±0.008	0.025±0.002	20±4	1.346	2.7(+0.1/−0.1)

Despite limitations imposed by the resolution of the method, an FI scan of a well- and coarsely laminated section of a massive stalagmite from Choranche reveals the potential value of high-resolution FI imaging. We have no data that allow us to infer that lamination occurs in annual cycles.

Fig. 10 shows the opposition of phases between fluorescence and reflectance for this coarsely (1 mm) laminated sample. The reflectance corresponds to a visible image of the calcite that is determined by the optical crystalline structure of calcite. The Fluorescence Index was measured with a 50-μm-wide slit at 20-μm step intervals. The colinear laser beam spot is about 3 mm in diameter. As a result, every part of the sample is exposed at the same time (the real-time bias of the protocol can be ignored). Comparing fluorescence intensity and Fluorescence Index reveals a global correlation with a lag of 60 μm for cross correlation. This shows that in this sample, a flush of OM (maximum fluorescence intensity) occurred before the change in the type of OM (FI maximum). As the lamination formation time is unknown, it is impossible to infer any environmental interpretation from this observation. Nevertheless, the fact that the variations in the quantity and type of OM in laminae are independent suggests that further high-resolution studies could provide interesting data on the flushing and storage of OM in karsts.

6.3. Calibration and comparison

In order to develop this work further, it will be necessary to combine the data obtained from FI scans with a detailed understanding of the storage of water and OM in karst environments. Such an understanding is fundamental to the accurate interpretation of stalagmite environmental and climatic records. Fluorescence Indices also need to be compared and calibrated with other isotopic and spectrometric data so that they can be used in practical environmental studies. Calibration will give a better knowledge of stalagmite fluorescence signatures and the modern-day environment. The FI scans of some well-known stalagmite records and the comparison of these indices with carbon isotope records are in progress to enable further palaeoenvironmental information to be extracted from the stalagmite record.

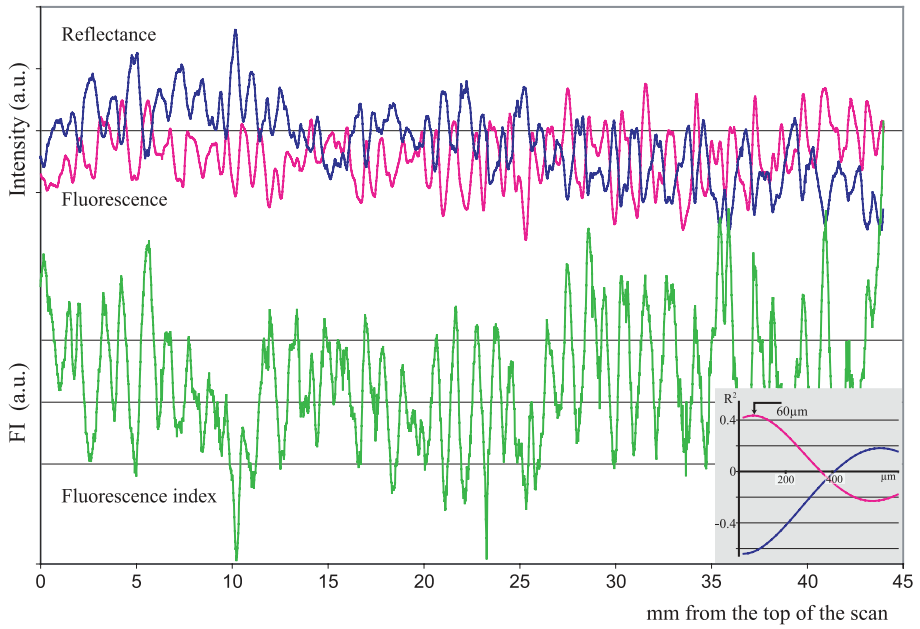

Fig. 10. Laminae Fluorescence Index (bottom), fluorescence and reflectance scan of a well-laminated stalagmite.

Acknowledgements

We would like to thank the "GDR 440" of the CNRS for the financial support it has provided since the beginning of this work. We would also like to thank the "Evolution passée du climat et de l'environnement en zone montagneuse" research program of the Mountain Institute in Chambery for its financial support. This work was initially developed at the Phlam laboratory and now continues at the EDYTEM laboratory; these two laboratories have provided us an excellent scientific environment to carry out our work.

Finally, we would like to thank Emmanuel Naffrechoux of the LCME (Molecular Chemistry and Environment Laboratory) for its critical review of this paper, as well as the reviewers for the journal. **[LW]**

References

Aitchison, J., Brown, J.A.C., 1969. The Lognormal Distribution. Cambridge University Press. 176 pp.

Baker, A., Brunsdon, C., 2003. Non-linearities in drip water hydrology: an example from Stump Cross Caverns, Yorkshire. J. Hydrol. 277 (3–4), 151–163.

Baker, A., Genty, D., 1999. Fluorescence wavelength and intensity variations of cave waters. J. Hydrol. 217 (1–2), 19–34.

Baker, A., Smart, P.L., Edwards, R.L., Richards, D.A., 1993. Annual growth banding in a cave stalagmite. Nature 364, 518–520.

Baker, A., Barnes, W.L., Smart, P.L., 1996. Speleothem luminescence intensity and spectral characteristics: signal calibration and a record of palaeovegetation change. Chem. Geol. 130, 65–76.

Berstad, I.M., Lundberg, J., Lauritzen, S.-E., Linge, H.C., 2002. Comparison of the climate during marine isotope stage 9 and 11 inferred from a speleothem isotope record from Northern Norway. Quat. Res. 58 (3), 361–371.

Borsato, A., 1997. Dripwater monitoring at Grotta di Ernesto (NE-Italy): a contribution to the understanding of karst hydrology and the kinetics of carbonate dissolution. Proc. 12th Int. Cong. Speleol., La Chaux-de-Fonds, vol. 2, pp. 57–60.

Bruckert, S., Gaiffe, M., 1989. Processus de formation et de fonctionnement des sols en relation avec le réseau poral des roches. Ann. Sci. Univ. Franche-Comté, Géol. 4 (9), 37–48.

Bruckert, S., Gaiffe, M., 1990. Les systèmes de subsurface sols-roches, modèles de pédogenèses. Exemple des domaines karstiques et non-karstiques de Franche Comté. Sci. Sol 28 (4), 319–332.

Chen, Y., Senesi, N., Schnitzer, M., 1977. Information provided on humic substances by E4/E6 ratios. Soil Sci. Soc. Am. J. 41, 352–358.

Chen, J., LeBoeuf, E.J., Dai, S., Gu, B., 2003. Fluorescence spectroscopic studies of natural organic matter fractions. Chemosphere 50 (5), 639–647.

Christ, M.J., David, M.B., 1996. Temperature and moisture effects on the production of dissolved organic carbon in a spodosol. Soil Biol. Biochem. 28 (9), 1191–1199.

Clapp, C.E., Hayes, M.H.B., 1999. Sizes and shapes of humic substances. Soil Sci. 164 (11), 777–789.

Clark, C.D., et al., 2002. A time-resolved fluorescence study of dissolved organic matter in a riverine to marine transition zone. Mar. Chem. 78 (2–3), 121–135.

Cook, R.L., Langford, C.H., 1995. Metal ion quenching of fulvic acid fluorescence intensities and lifetimes: nonlinearities and a possible three-component model. Anal. Chem. 67, 174–180.

Delannoy, J.J., Peiry, J.L., Destombes, J.L., Perrette, Y., 1999. Articulation des aspects ex-périmentaux, théoriques et méthodologiques de l'étude d'un système karstique à des fins environnementales: le laboratoire de Choranche. Proc. of Karst 99 Symposium, pp. 77–82.

Destombes, J.L., Cordonnier, M., Gadat, J.Y., Delannoy, J.J., 1997. Periodic and aperiodic forcing of water flow through sodastraw stalactites. Proc. 12th Int. Cong. Speleol., La Chaux-de-Fonds, vol. 2, pp. 69–73.

Donard, O.F.X., Lamotte, M., Belin, C., Ewald, M., 1989. High sensitivity fluorescence spectroscopy of Mediterranean waters using a conventional or a pulsed laser excitation source. Mar. Chem. 27, 117–136.

Fenart, P., 2002. Caractérisation du comportement hydromécanique des massifs rocheux fissurés. Thèse d'Université, Centre des matériaux de grande diffusion, Ecole des Mines d'Alès Thesis, Monpellier II, Montpellier. 308 pp.

Ford, D.C., Williams, P.W., 1989. Karst Geomorphology and Hydrology. Unwin Hymann, London. 601 pp.

Frappier, A., Sahagian, D., González, L.A., Carpenter, S.J., 2002. El Niño events recorded by stalagmite carbon isotopes. Science 18 (298), 565. (in Brevia).

Gaiffe, M., Bruckert, S., 1985. Analyse des transports de matière et des processus pédogenétiques impliqués dans les chaînes de sols du karst jurassien. Soil Geomorphol. Catena, Suppl. 6, 159–174.

Gascoyne, M., 1992. Paleoclimate determination from cave calcite deposits. Quat. Sci. Rev. 11, 609–632.

Genty, D., Deflandre, G., 1998. Drip flow variations under a stalactite of the Pere Noel cave (Belgium). Evidence of seasonal variations and air pressure constraints. J. Hydrol. 211 (1–4), 208–232.

Genty, D., Quinif, Y., 1996. Annually laminated sequences in the internal structure of some belgian stalagmites—importance for paleoclimatology. J. Sediment. Res. 66, 275–288.

Genty, D., Baker, A., Barnes, W., 1997. Comparison of annual luminescent and visible laminae in stalagmites. C. R. Acad. Sci., Sér. 2, Earth Planet. Sci. 325 (3), 193–200.

Genty, D., et al., 2001. Dead carbon in stalagmites: carbonate bedrock paleodissolution vs. ageing of soil organic matter. Implications for 13C variations in speleothems. Geochim. Cosmochim. Acta 65 (20), 3443–3457.

Genty, D., et al., 2002. Fossil water in large stalagmite voids as a tool for paleoprecipitation stable isotope composition reconstitution and paleotemperature calculation. Chem. Geol. 184 (1–2), 83–95.

Giralt, S., Klerkx, J., Riera, S., Julia, R., Lignier, V., Beck, C., De Batist, M., Kalugin, I., 2002. Recent paleoenvironmental evolution of Lake Issyk-Kul. In: Klerkx, J., Imanackunov, B. (Eds.), Lake Issyk-Kul: Its Natural Environment, Nato Science Series, IV. Earth and Environmental Sciences, vol. 13. Kluwer Academic Publishers, pp. 125–145. 286 pp.

Goede, A., 1994. Continuous early last glacial paleoenvironmental record from a Tasmanian speleothem based on stable isotope and minor element variations. Quat. Sci. Rev. 13, 283–291.

Hayase, K., Tsubota, H., 1985. Sedimentary humic acid and fulvic acid as fluorescent organic materials. Geochim. Cosmochim. Acta 49 (1), 159–163.

Hendy, C.H., 1971. The isotopic geochemistry of speleothems s.l. The calculation of the effect of different modes of formation on the isotopic composition of speleothems and their applicability as paleoclimatic indicators. Geochim. Cosmochim. Acta 35, 801–824.

Hill, C., Forti, P., 1997. In: NSS (Ed.), Cave Minerals of the World. 463 pp.

Jones, I.G., Indig, G.L., 1996. Spectroscopic and chemical bonding properties of humic acids in water. New J. Chem. 20, 221–232.

Kang, K.-H., Shin, H.S., Park, H., 2002. Characterization of humic substances present in landfill leachates with different landfill ages and its implications. Water Res. 36 (16), 4023–4032.

Kuczumow, A., Genty, D., Chevallier, P., Nowak, J., Ro, C.-U., 2003. Annual resolution analysis of a SW-France stalagmite by X-ray synchrotron microprobe analysis. Spectrochim. Acta, Part B: Atom. Spectrosc. 58 (5), 851–865.

Labview. 1999. National Instrument.

Lovlie, R., Moe, D., Ostbye, E., 1990. Paleoclimate deduced from a multidisciplinary study of a half million year old stalagmite from Rana, Northern Norway. Quat. Res., 34, 306–316.

Lepane, V., Persson, T., Wedborg, M., 2003. Effects of UV-B radiation on molecular weight distribution and fluorescence from humic substances in riverine and low salinity water. Estuar. Coast. Shelf Sci. 56 (1), 161–173.

Maroncelli, M., Fleming, G.R., 1987. Picosecond solvatation dynamics of coumarin 153: the importance of molecular aspects of solvatation. J. Chem. Phys. 86, 6221–6239.

Martin-Neto, L., Rosell, R., Sposito, G., 1998. Correlation of spectroscopic indicators of humification with mean annual rainfall along a temperate grassland climosequence. Geoderma 81, 305–311.

Mazhul, V.M., et al., 1997. Luminescence properties of humic substances. J. Appl. Spectrosc. 64, 503–508.

McDermott, F., et al., 1999. Holocene climate variability in Europe; evidence from $\delta^{18}0$, textural and extension-rate variations in three speleothems. Quat. Sci. Rev. 18, 1021–1038.

McGarry, S.F., Baker, A., 2000. Organic acid fluorescence: applications to speleothem paleoenvironmental reconstruction. Quat. Sci. Rev. 19, 1087–1101.

Miano, T.M., Senesi, N., 1992. Synchronous excitation fluorescence spectroscopy applied to soil humic substances chemistry. Sci. Total Environ. 117/118, 41–51.

Mobed, J.J., Hemmingsen, S.L., Autry, J.L., McGown, L.B., 1996. Fluorescence characterisation of IHSS humic substances: total luminescence spectra with absorbence correction. Environ. Sci. Technol. 30, 30610–30665.

Murton, J.B., et al., 2001. A late middle pleistocene temperate–periglacial–temperate sequence (Oxygen Isotope Stages 7–5e) near Marsworth, Buckinghamshire, UK. Quat. Sci. Rev. 20 (18), 1787–1825.

Perrette, Y., 2000. Etude de la structure interne des stalagmites : contribution à la connaissance géographique des évolutions environnementales du Vercors (France). Développement et application d'une approche multiparamètre des archives stalagmitiques. Thèse d'université Thesis, Université de Savoie, Chambery. 324 pp.

Perrette, Y., Genty, D., Destombes, J.L., Delannoy, J.J., Quinif, Y., 1997. Characterisation of speleothem crystalline fabrics by spectroscopic and digital image processing methods (Choranche, Vercors, France). Proc. 12th Int. Cong. Speleol., La Chaux-de-Fonds, vol. 1, pp. 257–260.

Perrette, Y., Delannoy, J.-J., Destombes, J.-L., 1999. Stratigraphic, image processing and spectroscopicstudies of some stalagmitic samples from the Vercors (France): preliminary results.. Proc. of Karst 99 Symposium, pp. 151–157.

Perrette, Y., et al., 2000. Comparative study of a stalagmite sample by stratigraphy, laser induced fluorescence spectroscopy, EPR spectrometry and reflectance imaging. Chem. Geol. 162, 221–243.

Perrette, Y., Delannoy, J.J., Destombes, J.L., Peiry, J.-L., 2001. Différents modes d'écoulement dans la zone vadose de Choranche. Actes du 7ème colloque d'hydrologie en pays calcaire et en milieu fissuré, pp. 269–272.

Peuravuori, J., Koivikko, R., Pihlaja, K., 2002. Characterization, differentiation and classification of aquatic humic matter separated with different sorbents: synchronous scanning fluorescence spectroscopy. Water Res. 36 (18), 4552–4562.

Quinif, Y., 1992. Datation uranium/thorium d'une séquence stalagmitique du pléistocène supérieur en Languedoc (Le couloir blanc, Grotte de Clamouse). J.C.R. Acad. Sci. Paris 314 (II), 1035–1042.

Ramseyer, K., et al., 1997. Nature and origin of organic matter in carbonates from speleothems, marine cements and coral skeletons. Org. Geochem. 26, 361–378.

Roberts, M.S., Smart, P.L., Baker, A., 1998. Annual trace element variations in a holocene speleothem. Earth Planet. Sci. Lett. 154, 237–246.

Rousseau, L., Bouloussa, O., Lumley (de), H.S., 1993. Evaluation de l'influence respective des acides humiques et des oxydes ferriques sur la coloration des planchers stalagmitiques. C.R. Acad. Sci., Paris 317, 367–370.

Sanger, J.L., Anderson, J.M., Little, D., Bolger, T., 1997. Phenolic and carbohydrate signatures of organic matter in soils developed under grass and forest plantation following changes in landse. Eur. J. Soil Sci. 48, 311–317.

Schnitzer, M., Khan, S.U., 1978. Soil Organic Matter. Elsevier. 316 pp.

Schrader, B., 1989. Raman/Infrared Atlas of Organic Compounds. Wiley, John and Sons.

Senesi, N., Miano, T.M., Provenzano, M.R., Brunetti, G., 1991. Characterisation differentiation and classification of humic substances by fluorescence spectroscopy. Soil Sci. 152, 259–271.

Shopov, Y.Y., Ford, D.C., Schwarcz, H.P., 1994. Luminescent microbanding in speleothems: high resolution chronology and paleoclimate. Geology 22, 407–410.

Siano, D.B., Metzler, D.E., 1969. Band shapes of the electronic spectra of complex molecules. J. Chem. Phys. 51, 1856–1861.

Spotl, C., Mangini, A., 2002. Stalagmite from the Austrian Alps reveals Dansgaard–Oeschger events during isotope stage 3: implications for the absolute chronology of Greenland ice cores. Earth Planet. Sci. Lett. 203 (1), 507–518.

Stevenson, F.J., 1994. Humus Chemistry: Genesis, Compositions, Reactions. Wiley, New York.

Van Beynen, P., Ford, D., Schwarcz, H., 2000. Seasonal variability in organic substances in surface and cave waters at Marengo Cave, Indiana. Hydrol. Process. 14, 1177–1197.

Van Beynen, P., Bourbonniere, R., Ford, D., Schwarcz, H., 2001. Causes of colour and fluorescence in speleothems. Chem. Geol. 175 (3–4), 319–341.

Verheyden, S., Keppen, E., Quinif, Y., Genty, D., 1999. Holocene palaeoclimatic and palaeo-environmental reconstruction inferred from stable isotopic and geochemical studies in Belgian caves and tunnels. Proceedings of the "Karst 99" Symposium (Mende, September 10–15), pp. 202–208.

White, W.B., 1981. Reflectance spectra and colour in speleothems. NSS Bull. 43, 20–26.

White, W.B., Brenan, E.S., 1989. Luminescence of speleothems due to fulvic acid and other activators. Proc. 10th Int. Cong. Speleol., Budapest, vol. 1, pp. 212–214.

Zech, W., et al., 1997. Factors controlling humification and mineralisation of soil organic matter in the tropics. Geoderma 79, 117–161.

Zepp, R.G., Schlotzhauer, P.F., 1981. Comparison of photochemical behavior of various humic substances in water: III. Spectroscopic properties of humic substances. Chemosphere 10, 479–486.